Dissolution Behavior and Hydrate Effect on CO₂ Ocean Sequestration

Namjin Kim

Mechanical Engineering Research Institute, Inha University
253 Yonghyun-dong, Nam-gu, Incheon 402-751, Korea

Chongbo Kim*

Department of Mechanical Engineering, Inha University,
253 Yonghyun-dong, Nam-gu, Incheon 402-751, Korea

CO₂ ocean sequestration is one of the promising options to reduce CO₂ concentration in the atmosphere because the ocean has vast capacity for CO₂ absorption. Therefore, in the present investigation, calculations for solubility and dissolution behavior of liquid CO₂ droplets released at 1000 m and 1500 m deep in the ocean from a moving ship and a fixed pipeline have been carried out in order to estimate the CO₂ dissolution characteristics in the ocean. The results show liquid CO₂ becomes CO₂ bubble at around 500 m in depth, and the solubility of seawater is about 5% less than of pure water. Also, it is shown that the injection of liquid CO₂ from a moving ship is a more effective method for dissolution than from a fixed pipeline, and the presence of hydrate on liquid CO₂ acts as a resistant layer in dissolving liquid CO₂.

Key Words : Global Warming, CO₂ Sequestration, Solubility, Hydrate, Dissolution

Nomenclature

A : Surface area of a CO₂ droplet [m²]
B : Buoyancy [kg/sec²]
b : Plume half width [m]
C_D : Drag coefficient
C_m : Centerline CO₂ concentration of plume [kg/m³]
C_o : Surface concentration with hydrate [kg/m³]
C_s : Solubility of CO₂ without hydrate [kg/m³]
C_w : Concentration of CO₂ volume per unit plume volume [kg/m³]
C_∞ : Ambient CO₂ concentration of a droplet [kg/m³]
D : Diffusion coefficient [m²/s]
D_n : Diameter of release port [m]

d_{CO_2} : Diameter of a CO₂ droplet [m]
d_{rel} : Droplet diameter at release point [m]
d_z : Droplet diameter at depth z [m]
f_{CO_2} : Fugacity of CO₂ [MPa]
g : Gravitational acceleration [m/sec²]
k : Mass transfer coefficient [m/s]
K_H : Henry's law constant [MPa]
M : Moment [kg·m/sec]
$M_{s,w}$: Molecular weight of seawater (CO₂ free) [kg/kmole]
P : Pressure [MPa]
q_z : CO₂ volume flux at depth z [m³/sec]
q_{rel} : CO₂ volume flux at release depth [m³/sec]
R : Radial distance from plume centerline [m]
R_e : Reynolds number
S : Salinity [‰]
Sc : Schmidt number
Sh : Sherwood number
T : Temperature [K]
U : Rising velocity of a CO₂ droplet [m/sec]
U_s : Velocity of the surrounding seawater [m/sec]
V : Volume of a CO₂ droplet [m³]

* Corresponding Author,
 E-mail : cbkim@inha.ac.kr
 TEL : +82-32-860-7313; **FAX** · +82-32-868-1716
 Department of Mechanical Engineering, Inha University, 253 Yonghyun-dong, Nam-gu, Incheon 402-751, Korea (Manuscript **Received** November 9, 2004; **Revised** March 29, 2005)

W : Local mean plume velocity [m/sec]

W_m : Centerline velocity of plume [m/sec]

x_{CO_2} : Solubility as a mole fraction

y : Distance from release point [m]

z : Ocean depth [m]

α : Salting-out coefficient

β : Entrainment coefficient

γ : Momentum amplification factor

ε : Effect factor of the hydrate

λ_1 : Spreading ratio of CO_2 volume flux to U

λ_2 : Spreading ratio of $\Delta\rho_w$ to U

$\mu_{s,w}$: Viscosity of seawater [N·sec/m²]

$\nu_{s,w}$: Kinematic viscosity of seawater [m²/sec]

ρ_a : Ambient CO_2 concentration of plume [kg/m³]

ρ_{CO_2} : Local CO_2 density [kg/m³]

ρ_{mix} : Density of plume [kg/m³]

ρ_{ref} : Ambient seawater density of release point [kg/m³]

$\rho_{s,w}$: Seawater density [kg/m³]

ρ_w : Local density of seawater within the plume [kg/m³]

$\varPhi$: Dimensionless association factor of seawater

Fig. 1 CO₂ released from pipeline hanged from a moving ship
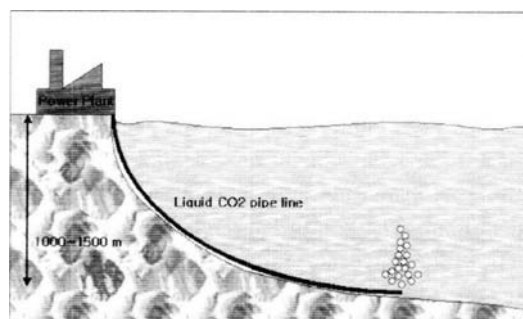
Fig. 2 CO₂ released from a fixed pipeline

1. Introduction

The idea of CO₂ sequestration in the ocean is proposed as an effective mitigation strategy to counteract potential global warming due to the "greenhouse effect" (Marchetti, 1977 ; Steinberg et al., 1984). CO₂ ocean disposal can be classified into two categories. One is the dissolution of CO₂ at an intermediate depth from a moving ship (Fig. 1) or a fixed pipeline (Fig. 2). The other is the storage of CO₂ in a seabed deeper than 3,000 m (Fig. 3). However the former can be more practical technology than the later from the pipeline design and the economical point of view (Fujioka et al., 1997).

In order to evaluate CO₂ disposal at an intermediate depth, Aya et al.(1992) and Shindo et al.(1995) investigated the shrinkage of hydrate-coated and hydrate-free CO₂ drops resting on a solid plate or a wire grid immersed in quiescent water or seawater. And Nishikawa et al.(1995) and Hirai et al.(1996 ; 1997) performed similar
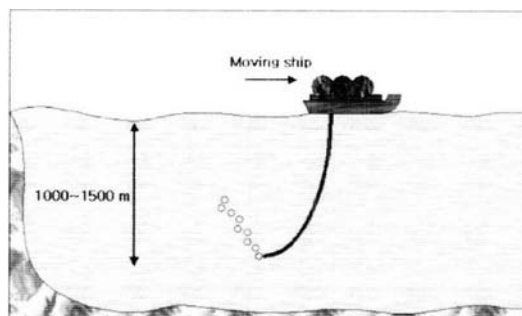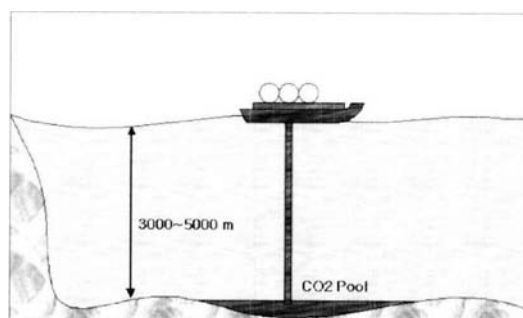

Fig. 3 Deep ocean storage of CO₂

observations with CO₂ drops, each held stationary by a basket or wire ring in steady, nearly parallel flow of seawater or pure water. Also Herzog et al.(1996) observed the environmental impacts of the ocean disposal of CO₂. Teng et al. (1996) attempted to assess the effect of the variation of solubility along depth on the dissolution of CO₂ effluent, and Kim et al.(2000) predicted the dissolution behavior of a CO₂ single droplet in the ocean.

However, most of the previous researchers attempted to predict the CO_2 dissolution behavior by utilizing the physical and chemical properties of pure water and neglecting the effect of hydrate formed at the interface between a CO_2 droplet and seawater as shown in Fig. 4. Also they calculated the dissolution behavior by assuming that the solubility and the salinity are constant along the depth. In order to make CO_2 drops dissolve completely in the ocean, it is important to predict the CO_2 dissolution behavior along the depth accurately. Therefore, the simplistic property data utilized in previous research could give inaccurate predictions.

A more realistic modelling for property data is adapted in the present investigation from a location point in Clipperton-clarion as a CO_2 sequestration spot which was assigned to the Republic of Korea by the United Nations for seabed mining. The solubility relationship of liquid CO_2 without hydrate both in pure water and in seawater also and the dissolution behavior of CO_2 released from a moving ship and a fixed pipeline at an intermediate ocean depth are being calculated utilizing real properties data from Clipperton-clarion. The effect of hydrate formed at the interface between a CO_2 droplet and seawater are also being investigated.
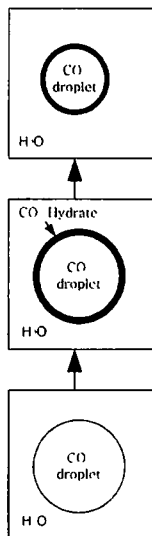

Fig. 4 Formation of CO_2 hydrate in water

2. Numerical Model

2.1 Solubility of liquid CO_2 droplet without hydrate surface

Liquid CO_2 and seawater are very dissimilar. liquid CO_2 is a nonpolar substance, while seawater has strong polarity. Therefore, the solubility of liquid CO_2 in seawater is much larger than that of seawater in liquid CO_2. In the present investigation, the liquid CO_2-seawater system is treated as one-sided solubility system assuming liquid CO_2 as the solute and seawater as the solvent. The solubility (C_s) of CO_2 without hydrate coating may be expressed as follows (Teng et al., 1996 ; Teng and Yamasaki, 1998) :

$$C_s = \frac{x_{CO_2}\rho_{s,w}}{(1-x_{CO_2})M_{s,w}} \times \left(\frac{44 \text{ kg}}{1 \text{ kmol}}\right) \quad (1)$$

where the solubility (x_{CO_2}) of CO_2 in a mole fraction is expressed by the modified Henry's law (King, 1969).

$$x_{CO_2} = \frac{f_{CO_2}}{K_H} \quad \text{in pure water} \quad (2)$$

$$= \left(\frac{f_{CO_2}}{K_H}\right) e^{\alpha S x_w} \quad \text{in seawater} \quad (3)$$

In the calculation, the Henry's law constant, K_H and the salting-out coefficient, α by Teng and Yamasaki (1998) are being utilized.

2.2 Dissolution behavior of CO_2 droplet

2.2.1 Moving ship model

As shown in Fig. 1, a CO_2 droplet rises upward due to buoyancy when it is released at the intermediate depth in the ocean from a moving ship. Therefore, the dissolution behavior of a single droplet can be described as

$$\frac{d}{dt}(\rho_{CO_2}V) = -kA(C_o - C_\infty) \quad (4)$$

$$\frac{d}{dt}(d_{CO_2}) = -\frac{2k(C_o - C_\infty)}{\rho_{CO_2}} - \frac{d_{CO_2}}{3\rho_{CO_2}} \cdot \frac{d\rho_{CO_2}}{dt} \quad (5)$$

where

$$\frac{d}{dt}(d_{CO_2}) = \frac{dd_{CO_2}}{dz} \cdot \frac{dz}{dt} = \frac{dd_{CO_2}}{dz}(U - U_s) \quad (6)$$

$$\frac{d}{dt}(\rho_{CO_2}) = \frac{d\rho_{CO_2}}{dz} \cdot \frac{dz}{dt} = \frac{d\rho_{CO_2}}{dz}(U - U_s) \quad (7)$$

Therefore, Eq. (5) can be modified to calculate the change in diameter of CO_2 droplet in a function of depth, z :

$$\frac{d(d_{CO_2})}{dz} = -\frac{2k(C_o - C_\infty)}{(U - U_s)\rho_{CO_2}} - \frac{d_{CO_2}}{3\rho_{CO_2}} \frac{d(\rho_{CO_2})}{dz} \quad (8)$$

In a pure single droplet model, $U_s = 0$ and if $C_o \gg C_\infty$, we may make the approximation that $C_o - C_\infty = C_o$.

According to Hirai (1996 ; 1997) and Mori (1998), the CO_2 droplet behaves like a rigid sphere because of the hydrate on the surface in the actual situation, and it is suggested that the mass transfer coefficient, k is obtained from

$$Sh = 1 + 0.752\left(Sc + \frac{1}{Re}\right)^{1/3} Re^{0.477} \quad (9)$$

and the slip velocity, U and the diffusion coefficient, D are described from Clift et al.(1978), and Wilke and Chang (1955) to be

$$U = \sqrt{\frac{4d_{CO_2}(\rho_{s,w} - \rho_{CO_2})g}{3C_D\rho_{s,w}}} \quad (10)$$

$$D = \frac{7.4 \times 10^{-8}(\Phi M_{s,w})^{0.5} T}{\mu_{s,w} V_{CO_2}^{0.6}} \quad (11)$$

2.2.2 Fixed pipeline model

As shown in Fig. 2, when the liquid CO_2 is released in the ocean from a fixed pipeline, the droplets form a plume like Fig. 5. Therefore, from Eq. (9), the maximum concentration (C_m) and the velocity (W_m) in the plume can be obtained in the following equation (Morton et al., 1956 ; Clift et al., 1978 ; Liro et al., 1992) :

$$\frac{d(d_{CO_2})}{dz} = -\frac{2k(C_o - C_m)}{(U + W_m)\rho_{CO_2}} - \frac{d_{CO_2}}{3\rho_{CO_2}} \frac{d(\rho_{CO_2})}{dz} \quad (12)$$

And CO_2 volume flux (q_z) along the ocean depth can be expressed as

$$q_z = q_{rel}\left(\frac{d_z}{d_{rel}}\right)^3_{CO_2} = \int_R 2\pi C_w(U + W)RdR \quad (13)$$

where the velocity (W) and the concentration (C_w) profile are given

$$W = W_m e^{(-R^2/b^2)} \quad (14)$$
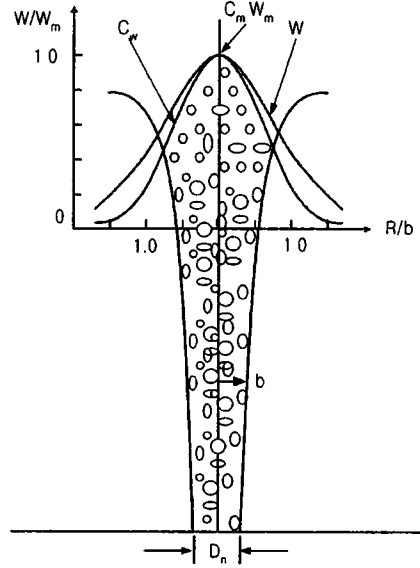
$$C = C_m e^{(-R^2/\lambda_1 b^2)} \quad (15)$$

Fig. 5 Schematic of a plume

Substituting Eqs. (15) and (16) into Eq. (14), the equation for C_m is expressed as

$$C_m = \frac{\dfrac{q_z}{\pi b^2 \lambda_1}}{W_m \dfrac{1}{1 + \lambda_1^2} + U} \quad (16)$$

The expression for the liquid volume flux (Q) is also obtained to be

$$Q = \int_0^\infty (1 - C_w)2\pi WRdR \approx \int_0^\infty 2\pi WRdR \\ = \pi W_m b^2 \quad (17)$$

The rate of entrainment of ambient water into the plume is established with the assumption that the entrainment velocity (W_e) is proportional to the centerline velocity.

$$W_e = \beta W_m \quad (18)$$

Thus the conservation of liquid volume implies

$$\frac{dQ}{dy} = 2\pi b W_e = 2\pi \beta b W_m$$

$$\frac{d}{dy}(W_m b^2) = 2\beta b W_m \quad (19)$$

Since buoyancy force (B) is assumed to be the only force acting upon the plume, the momentum of the plume is defined as follows (Rayyan, 1974) :

$$\frac{dM}{dy} = B_y$$

$$\frac{d}{dy} \int_0^\infty 2\pi\gamma W^2 \rho_{ref} R dR = \int_0^\infty 2\pi g (\rho_a - \rho_{max}) R dR \qquad (20)$$

where

$$\rho_a = \rho_w - \Delta\rho_{w,m} e^{-R^2/(\lambda_2 b)^2} \qquad (21)$$

$$\rho_{max} = C_w \rho_{CO_2} + (1 - C_w) \rho_w \qquad (22)$$

Substituting Eqs. (21) and Eq. (23) into Eq. (20), the following equation can be obtained

$$\frac{d}{dy}(b^2 W_m^2) = \frac{2gb^2}{\gamma} \left(C_m\lambda_1^2 \frac{\rho_w - \rho_{CO_2}}{\rho_{ref}} - \lambda_2^2 \frac{\Delta\rho_{w,m}}{\rho_{ref}} \right) \quad (23)$$

Also, from Eqs. (20) and (25), the following equations are being obtained

$$\frac{d}{dy}(W_m) b^2 + 2bW_m\frac{db}{dy} = 2\beta b W_m$$

$$\frac{db}{dy} = \beta - \frac{b}{2W_m}\frac{dW_m}{dy} \qquad (24)$$

$$2W_m b^2 \frac{dW_m}{dy} + 2bW_m^2\frac{db}{dy}$$

$$= \frac{2gb^2}{\gamma} \left(C_m\lambda_1^2 \frac{\rho_w - \rho_{CO_2}}{\rho_{ref}} - \lambda_2^2 \frac{\Delta\rho_{w,m}}{\rho_{ref}} \right) \qquad (25)$$

Then, substituting Eq. (24) into Eq. (25), the maximum velocity and the half width (b) of the plume can be expressed as a function of depth.

$$\frac{dW_m}{dz} = -\frac{2g}{\gamma W_m} \left(C_m\lambda_1^2 \frac{\rho_w - \rho_{CO_2}}{\rho_{ref}} - \lambda_2^2 \frac{\Delta\rho_{w,m}}{\rho_{ref}} \right) + \frac{2\beta W_m}{b} \quad (26)$$

$$\frac{db}{dz} = -2\beta + \frac{gb}{\gamma W_m^2} \left(C_m\lambda_1^2 \frac{\rho_w - \rho_{CO_2}}{\rho_{ref}} - \lambda_2^2 \frac{\Delta\rho_{w,m}}{\rho_{ref}} \right) \quad (27)$$

If the right hand side of Eq. (28) becomes

$$C_m\lambda_1^2 \frac{\rho_w - \rho_{CO_2}}{\rho_{ref}} < \lambda_2^2 \frac{\Delta\rho_{w,m}}{\rho_{ref}} \qquad (28)$$

a peeling of the seawater from the plume occurs, and the buoyancy force caused by the stratification of ambient seawater density may be expressed as

$$B_w = \int_0^\infty 2\pi (\rho_{ref} - \rho_w) R dR \qquad (29)$$

$$\frac{d}{dy} \int_0^\infty 2\pi W (\rho_{ref} - \rho_w) R dR = 2\pi b\beta W_m (\rho_{ref} - \rho_a) \quad (30)$$

Substituting Eqs. (14), (19), and (21) into Eq. (30), the Eq. (30) changes to be Eq. (31) in terms of depth :

$$\frac{d}{dz}\Delta\rho_{w,m} = -\frac{1+\lambda_2^2}{\lambda_2^2}\frac{d\rho_a}{dz} + \frac{2\beta\Delta\rho_{w,m}}{b} \qquad (31)$$

3. Results and Discussions

In the present investigation, it is assumed that 10 m difference in ocean depth corresponds to 0.1 MPa pressure difference. The density of pure liquid carbon dioxide (ρ_{CO_2}) and the fugacity (f_{CO_2}) are obtained from REFPROP 6.01 by the National Institute of Standards and Technology (NIST). On the other hand, the density ($\rho_{s,w}$), the kinematic viscosity ($\nu_{s,w}$), the temperature and the salinity ($S‰$) according to the ocean depth at Clipperton-clarion are available from the IRI/LDEO Climate Data Library in Columbia University. The densities of pure liquid CO_2 at different temperatures and pressures along the ocean depth at Clipperton-clarion are shown in Fig. 6.

3.1 Solubility of liquid CO₂ droplet without hydrate coating

Figure 7 shows the solubility of liquid CO_2 droplet without hydrate surface in pure water and seawater calculated by substituting Eqs. (2) and (3) into Eq. (1). It is found that the solubility of CO_2 in seawater is lower than that in pure water.
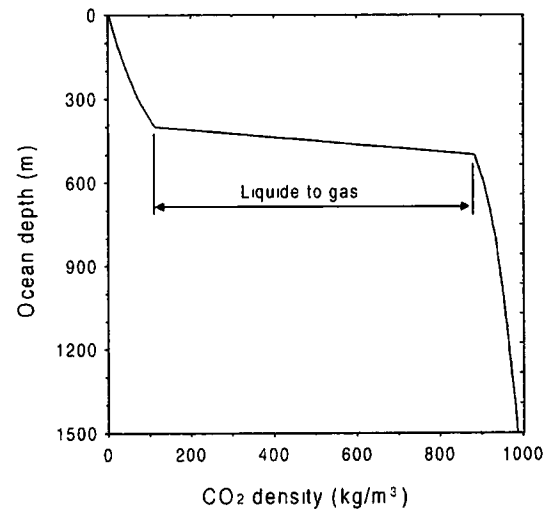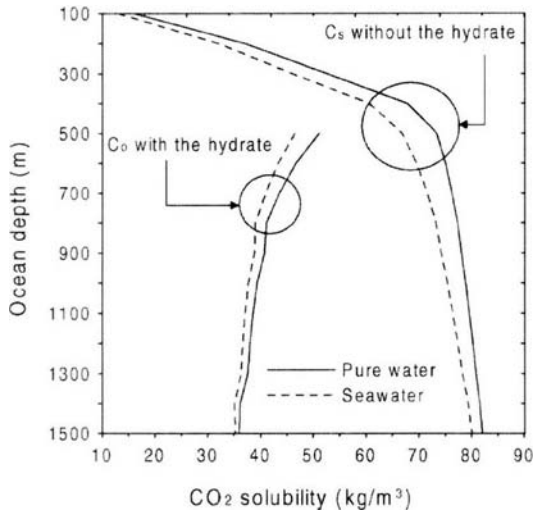

Fig. 6 Density distributions of liquid CO_2 along depth

Fig. 7 Solubility distributions of liquid CO_2 without the hydrate along depth

Fig. 8 Surface concentration of a CO_2 droplet with the hydrate in pure water

If the difference is averaged for the depth in the range of 500 m to 1500 m, the relationship in solubilities between seawater and pure water is expressed as
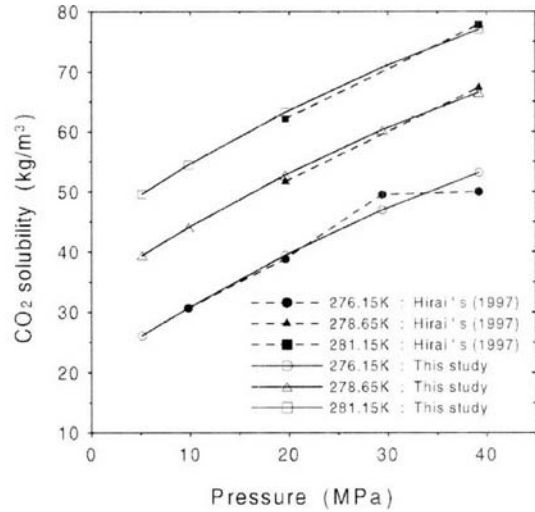
$$C_s \ (in \ seawater) = 0.95 C_s \ (in \ pure \ water) \atop (500 \leq z \leq 1500) \quad (32)$$

The sudden changes in the gradient of the solubility of liquid CO_2 are observed around at 500 m in depth. The solubility of liquid CO_2 increases at an average rate of 0.1349 kg/m^3 per meter from 100 m to 500 m. On the other hand, the increasing rate of the solubility from 500 m to 1500 m significantly decreases at 0.0132 kg/m^3 per meter, which is only one tenth of the former one. In addition, it is found as in Figs. 6 and 7 liquid CO_2 droplet turns to be CO_2 bubble in gas phase at around 500 m in depth. Then, CO_2 quickly escapes to the atmosphere if a liquid CO_2 droplet does not completely dissolve in seawater under 500 m or below. Therefore, in order to ensure CO_2 not escaping to the atmosphere, it is important to ensure CO_2 dissolve completely at the depth of 500 m or below in the ocean.

3.2 Solubility of liquid CO_2 with hydrate coating

The most important characteristic of CO_2 sequestration in the ocean is the formation of

a hydrate at the interface between seawater and liquid CO_2 droplet (Fig. 4) so that the solubility, C_o of a liquid CO_2 droplet with hydrate coating is quite different from the solubility, C_s of liquid CO_2 without hydrate coating. With this fact in consideration, experimental data for the solubility are obtained by Hirai et al. (1997). For engineering applications, these experimental data give the following formula for C_o in terms of temperature (K) and pressure (MPa).

$$C_o = a + b \times P + c \times P^2 + \alpha \times T + \beta \times T^2$$
$$a = -1.95 \times 10^4, \ b = 1.08, \ c = -6.51 \times 10^{-3} \quad (33)$$
$$\alpha = 135, \ \beta = -2.34 \times 10^{-1}$$

The calculated and Hirai's data (1997) in pure water are shown in Fig. 8. It is shown that calculated results are in good agreement with experimental results. Also, using Eqs. (32) and (33), the solubility, C_o of a liquid CO_2 droplet with hydrate is calculated and presented in Fig. 7. If the prediction formula is introduced in estimating CO_2 dissolution behavior, it can be possible to predict the solubility of CO_2 with the hydrate coating without carrying experimentations.
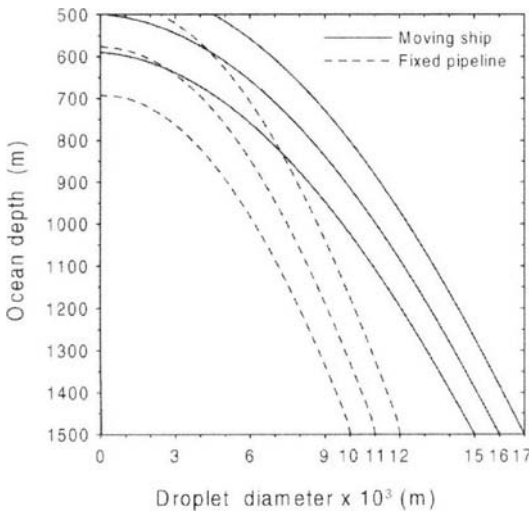
3.3 Dissolution behavior

Figures 9 and 10 show the dissolution behavior of CO_2 where the droplet is released at 1,000 m
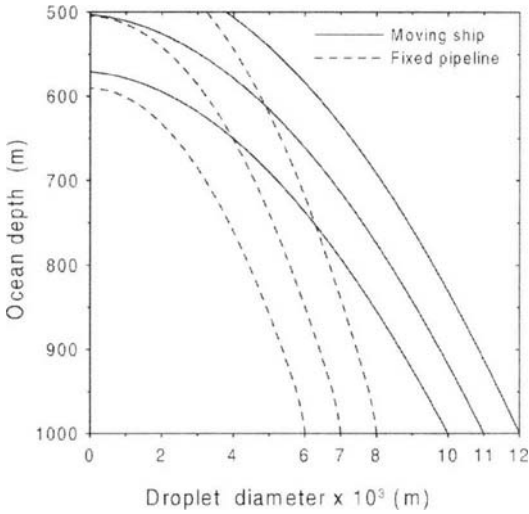
Fig. 9 Dissolution behavior of the CO_2 droplets with the hydrate released in seawater of 1,000 m in depth
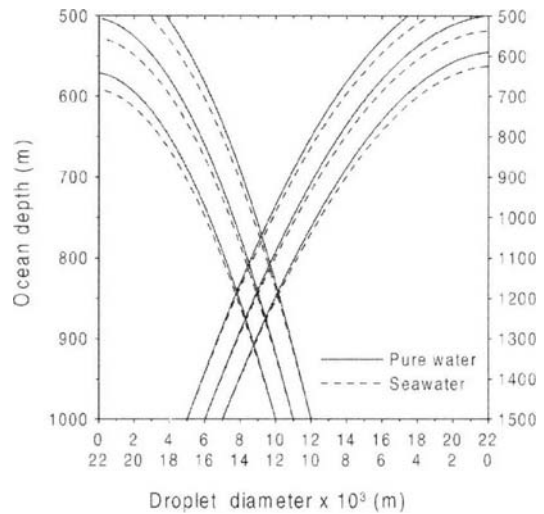
Fig. 11 Dissolution behavior of a CO_2 droplet with the hydrate released from a moving ship

**Fig. 10** Dissolution behavior of the CO_2 droplets with the hydrate released in seawater of 1, 500 m in depth

and 1,500 m in depth and rises up to 500 m from a moving ship and a fixed pipeline with the flow rate of 133 kg/s, $\beta=0.1$, $\lambda_1=0.8$, $\lambda_2=1.25$, and $\gamma=1.0$ (Milgram, 1983; Rayyan, 1974). It is shown that the droplet is completely dissolved before they reach 500 m deep in the ocean, if the initial CO_2 droplet diameter is of 0.011 m or smaller at 1,000 m depth and 0.016 m or smaller

at 1,500 m depth from a moving ship. However, the initial droplet diameters for a complete dissolution should be 0.007 m or less at 1,000 m depth and 0.011 m or less at 1,500 m depth from a fixed pipeline, respectively. Therefore, the initial droplet size is the key parameter in the dissolution of liquid CO_2 released at the intermediate depth in the ocean. It can be also concluded that the injection of liquid CO_2 from a moving ship can be more effective means than from a fixed pipeline. Also, if the dissolution behavior is calculated in pure water, the error is found to be 5% as shown in Fig. 11.
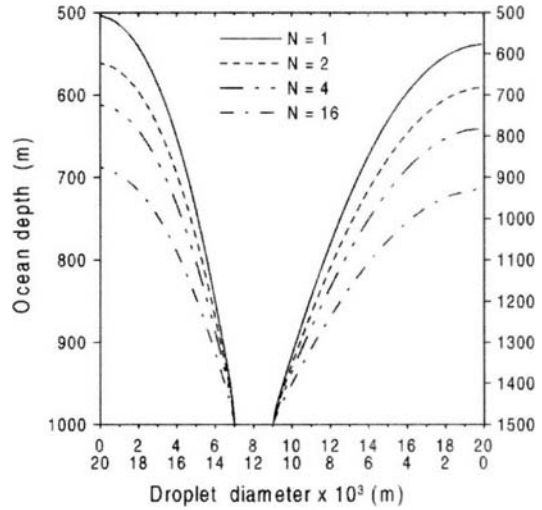
The CO_2 droplets injected from a fixed pipeline form a plume as shown in Figs. 12 and 13, and the plume repeat the expansion and the shrinking due to the peeling. Also, Fig. 14 shows the dissolution behavior of CO_2 on the increase of the injection port at constant initial droplet diameters and constant flow rates. It is obvious that more ports ensure faster CO_2 dissolution. However, the ocean depth for a complete dissolution of the droplets does not decrease in spite of increasing numbers of injection ports.
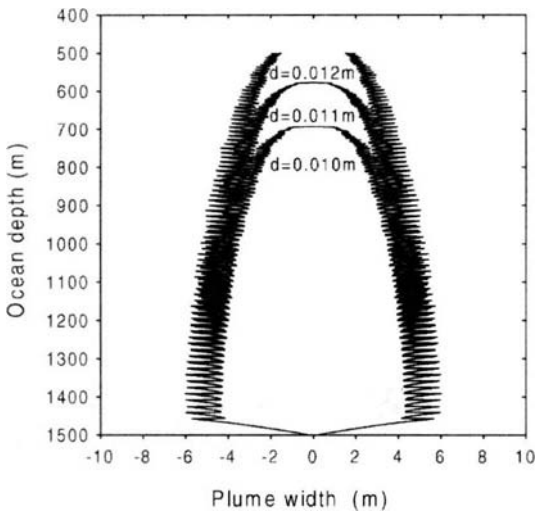
3.4 Hydrate coating effects

In the present investigation, it is proposed that the hydrate effects are expressed in the following
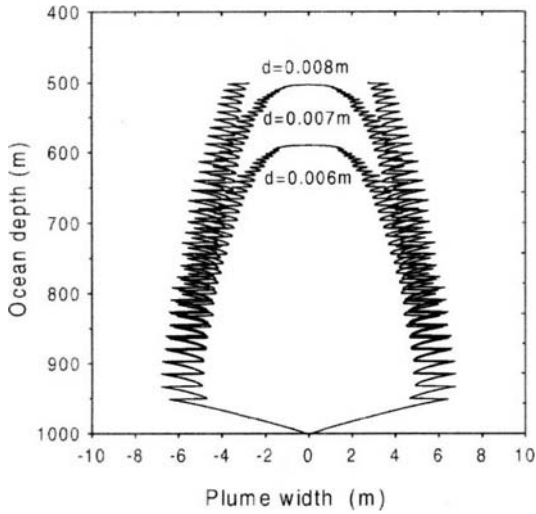
Fig. 12 Plume width (2b) on the CO_2 droplets released at 1,000 m in depth from a fixed pipeline

Fig. 13 Plume width (2b) on the CO_2 droplets released at 1,500 m in depth from a fixed pipeline

form

$$C_o = \varepsilon C_s \qquad (34)$$

According to the results of Hirai et al. (1996), ε is found to be about 0.5 at 10~40 MPa at 276 K. However, it is found as in Fig. 15 that ε becomes 0.6, not 0.5 if the droplet is released at 1,000 m below. And, if it is released at 1,500 m, ε cor-

Fig. 14 Effect of number of nozzles on the CO_2 droplets released from a fixed pipeline
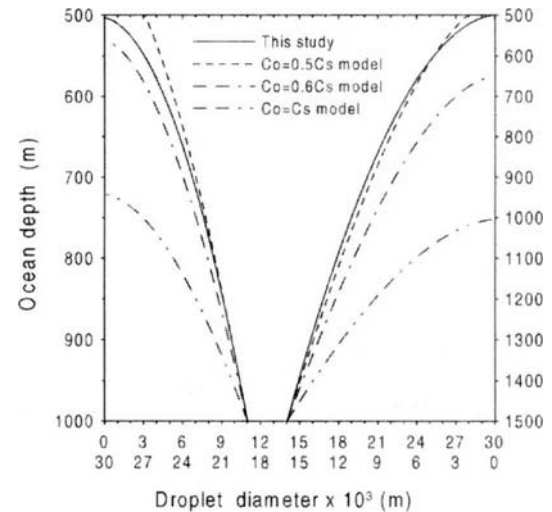
Fig. 15 Effect of hydrate on CO_2 dissolution behavior released from a moving ship

responds to 0.5 according to the results of Hirai et al. (1996). Therefore, the different values of ε should be applied for an accurate prediction depending on the releasing depth. Also, it is shown that the hydrate on the droplet surface acts as an obstacle for the dissolution in seawater. If the hydrate formation is neglected, it gives a poor prediction for the CO_2 dissolution.

Liquid CO_2 turns to be CO_2 bubbles at the depth of around 500 m in the ocean, and the

solubility in seawater is found to be about 95% of the pure water.

(2) The prediction formula in terms of temperature and pressure utilized in engineering applications is being proposed, and the surface concentration of carbon dioxide with the hydrate coating can be predicted without carrying experimentations.

(3) The solubility of CO_2 droplet with hydrate coating is approximately 60% and 50% of CO_2 solubilities without hydrate coating at 1,000 m and 1,500 m in depth, respectively. Therefore, the hydrate acts as a barrier for the dissolution of liquid CO_2 in the ocean and the hydrate effect should be included at each different ocean depth.

(4) The initial CO_2 droplet diameter is of 0.011 m or smaller at 1,000 m depth and 0.016 m or smaller at 1,500 m depth from a moving ship. However, the initial droplet diameters for a complete dissolution should be 0.007 m or less at 1,000 m depth and 0.011 m or less at 1,500 m depth from a fixed pipeline, respectively. Therefore, the initial droplet size is the key parameter in the dissolution of liquid CO_2 released at the intermediate depth in the ocean.

(5) The injection of liquid CO_2 from a moving ship can be more effective means than from a fixed pipeline. Also, if the dissolution behavior is calculated in pure water, the error is found to be 5%.

(6) The plume repeat the expansion and the shrinking due to the peeling, and the ocean depth for a complete dissolution of the droplets does not decrease in spite of increasing numbers of injection ports.

Acknowledgments

References

Aya, I., Yamane, K. and Yamada, N., 1992, "Stability of Clathrate-hydrate of Carbon Dioxide in Highly Pressurized Water," *ASME HTD*, Vol. 215, pp. 17~22.

Clift, R., Grace, J. R. and Weber, M. E., 1978, *Bubbles, Drops and Particles*, Academic Press, pp. 97~125.

Fujioka, Y., Ozaki, M., Takeuchi, K., Shindo, Y. and Herzog, H. J., 1997, "Cost Comparison in Various CO_2 Ocean Disposal Option," *Energy Convers. Mgmt.*, Vol. 38, pp. s273~s277.

Herzog, H. J., Adams, A. A., Auerbach, A. and Caulfield, J., 1996, "Environmental Impacts of Ocean Disposal of CO_2," *Energy Convers. Mgmt.*, Vol. 37, No. 6-8, pp. 999~1005.

Hirai, S., Okazaki, K., Araki, Yazawa, H., Ito, H. and Hijikata, K., 1996, "Transport Phenomena of Liquid CO_2 in Pressurized Water Flow with Clathrate-hydrate at the Interface," *Energy Convers. Mgmt.*, Vol. 36, No. 6-8, pp. 489~492.

Hirai, S., Okazaki, K., Tabe, Y., Hijikata, K. and Mori, Y., 1997, "Dissolution Rate of Liquid CO_2 in Pressurized Water Flows and the Effect of Clathrate Film," *Energy Convers. Mgmt.*, Vol. 22, No. 2-3, pp. 285~293.

Kim, N. J., Lee, J. Y., Hur, B. G., Seo, T. B. and Kim, C. B., 2000, "Dissolution Characteristics of Liquid CO_2 Injected at the Intermediate Depth of the Ocean," *KSME Int, J.*, Vol. 14, No. 11, pp. 1276~1285.

King, M. B., 1969, *Phase Equilibrium in Mixtures*, Pergamon Press, London.

Liro, C. R., Adams, E. E. and Herzog, H. J., 1992, "Modeling the Release of CO_2 in the Deep Ocean," *Energy Convers. Mgmt.*, Vol. 33, No. 5-8, pp. 667~674.

Marchetti, C., 1977, "On Geoengineering and CO_2 Problem," *Climate Change*, Vol. 1, pp. 59~68.

Milgram, J. H., 1983, "Mean Flow in Round Bubble Plumes," *J. of Fluid Mechanics*, Vol. 133, pp. 345~376.

Mori, Y. H. and Mochizuki, T., 1998, "Dissolution of Liquid CO_2 into Water at High Pressures : a Search for the Mechanism of Dissolution Being Retarded Through Hydrate-film Formation," *Energy Convers. Mgmt.*, Vol. 39, No. 7, pp. 569~578.

Morton, B. R., Taylor, G. I. and Turner, J. S., 1956, "Turbulent Gravitational Convection From Maintained and Instantaneous Sources," *Pro-

ceedings of the Royal Society, A234, pp. 1~23.

Nishikawa, N., Ishibashita, M., Ohta, H., Akutsu, N., Tajika, M., Sugitani, T., Hiraoka, R., Kimuro, H. and Moritoki, M., 1995, "Stability of Liquid CO₂ Spheres Covered with Clathrate Film When Exposed to Environment Simulating the Deep Sea," *Energy Convers. Mgmt.*, Vol. 36, pp. 489~492.

Rayyan, F. M., 1974, "Hydrodynamics of Bubble Plumes Incorporating Gas Transfer in Stratified Impoundments," *Ph.D. Dissertation*, The University of Texas at Austin.

Shindo, Y., Fujikoka, Y., Yanagishita, Y., Hakuta, T. and Komiyama, H., 1995, "Formation of stability of CO₂ hydrate," *Direct Ocean Disposal of CO₂*, Terrapub, Tokyo, Japan, pp. 217~223.

Steinberg, M., Cheng, H. C. and Horn, F., 1984, "A Systems Study for Removal, Recovery and Disposal of CO₂ From Fossil Fuel Power Plants in U.S.," *Informal Report BNL 35666*, Brookhaven National Laboratory, Long Island, N.Y., U.S., pp. 42~58.

Teng, H., Masutani, S. M., Kinoshita, C. M. and Nohous, G. C., 1996, "Solubility of CO₂ in the Ocean and its Effect on CO₂ Dissolution," *Energy Convers. Mgmt.*, Vol. 37, No. 6-8, pp. 1029~1038.

Teng, H. and Yamasaki, A., 1998, "Solubility of Liquid CO₂ in Synthetic Seawater at Temperatures From 278K to 293K and Pressures From 6.44 MPa to 29.49 MPa, and Densities of the Corresponding Aqueous Solution," *J. Chem. Eng. Data*, Vol. 43, pp. 2~5.

Wilke, C. R. and Chang, P., 1995, "Correlation of Diffusion Coefficient in Dilute Solutions." *A.I.Ch. J.*, Vol. 1, pp. 264~270.